Long Range Allosteric Control of Cytoplasmic Dynein ATPase Activity by the Stalk and C-terminal Domains*⑤

Peter Höök‡, Atsushi Mikami‡[1], Beth Shafer‡, Brian T. Chait§, Steven S. Rosenfeld¶, and Richard B. Vallee‡¶[2]

From the ‡Department of Pathology and Cell Biology, Columbia University, New York, New York 10032, the §Laboratory of Mass Spectrometry and Gaseous Ion Chemistry, Rockefeller University, New York, New York 10022, and the ¶Department of Neurology, Columbia University, New York, New York 10032

The dynein motor domain consists of a ring of six AAA domains with a protruding microtubule-binding stalk and a C-terminal domain of unknown function. To understand how conformational information is communicated within this complex structure, we produced a series of recombinant and proteolytic rat motor domain fragments, which we analyzed enzymatically. A recombinant 210-kDa half-motor domain fragment surprisingly exhibited a 6-fold higher steady state ATPase activity than a 380-kDa complete motor domain fragment. The increased ATPase activity was associated with a complete loss of sensitivity to inhibition by vanadate and an ~100-fold increase in the rate of ADP release. The time course of product release was discovered to be biphasic, and each phase was stimulated ~1000-fold by microtubule binding to the 380-kDa motor domain. Both the half-motor and full motor domain fragments were remarkably resistant to tryptic proteolysis, exhibiting either two or three major cleavage sites. Cleavage near the C terminus of the 380-kDa motor domain released a 32-kDa fragment and abolished sensitivity to vanadate. Cleavage at this site was insensitive to ATP or 5′-adenylyl-β,γ-imidodiphosphate but was blocked by ADP-AlF₃ or ADP-vanadate. Based on these data, we proposed a model for long range allosteric control of product release at AAA1 and AAA3 through the microtubule-binding stalk and the C-terminal domain, the latter of which may interact with AAA1 to close the motor domain ring in a cross-bridge cycle-dependent manner.

Cytoplasmic dynein is a microtubule-based motor that utilizes energy from ATP hydrolysis to facilitate a wide variety of functions in eukaryotic cells such as spindle alignment, nucleus positioning and chromosome separation during mitosis, and retrograde axonal transport of subcellular components (1, 2). Dynein belongs to the functionally diverse family of AAA+ proteins (3). Members of this family contain a conserved domain of 200–250 residues termed AAA, or "ATPases associated with various cellular activities," that contains five signature motifs involved in ATP binding and hydrolysis. Most AAA proteins form homohexameric rings in which each subunit is composed of either one or two AAA domains. The ~380-kDa dynein motor, in contrast, consists of a ring of six dissimilar and covalently linked AAA domains and at the extreme C terminus an ~30-kDa region of unknown

function. Fused to the motor domain is a substantial projection, referred to as the stem, which contains sites for dimerization and association with cargo binding subunits (4). Emerging from between AAA4 and AAA5 is another projection, the stalk, which is thought to consist of an antiparallel coiled-coil with a globular domain for microtubule binding at its tip (5).

Sequence analysis of the dynein motor domain suggests that the ability to bind and hydrolyze nucleotides differs among the six AAA domains (6). Whereas the first AAA domain contains the entire set of nucleotide-interacting motifs, the probability of identifying these motifs in AAA2–AAA4 varies with organism and class of dynein. The AAA consensus in the fifth and sixth AAA domain are partly or entirely degenerate, making the C-terminal half of the ring incapable of nucleotide binding and hydrolysis. Based on vanadate photocleavage data, the first AAA domain has been designated the main site for ATP hydrolysis (5, 7), whereas the third AAA domain has emerged as a potential secondary site for hydrolysis (8, 9). The mechanism for coupled nucleotide hydrolysis and force production within the dynein motor is not fully understood. Microtubule binding by dynein sharply increases the rate of ATP hydrolysis (10), indicating a central role for the stalk in regulating enzymatic activity. Recent work on P-loop mutants showed that nucleotide binding at the first and third AAA domains is required for ATP-induced release of microtubules (11) and for microtubule stimulation of ATPase activity (8), supporting long range allosteric communication through unknown conformational changes within the motor domain. The complexity of dynein motor mechanics has been further reinforced by results from electron microscopy of an axonemal dynein, in which part of the stem was bent around the AAA ring in either of two conformations, depending on whether the motor was in a pre- or post-power stroke state (12).

To improve our understanding of how the motor activity in cytoplasmic dynein is regulated, we produced two fragments from the 4644-residue heavy chain and studied their properties. The first fragment corresponded to the entire 380-kDa motor domain, and the second to the N-terminal 210-kDa half of the motor domain (half-motor domain). Although both fragments contain the entire machinery for ATP hydrolysis, they unexpectedly display distinctive enzymatic properties. Most surprisingly, the ATPase activity and ADP release rate of the half-motor were considerably higher than those of the full motor. In addition, the 210-kDa fragment lost its sensitivity to inhibition by vanadate ion, a mimic of the γ-phosphate of ATP, and to photocleavage in the presence of vanadate. Each fragment was remarkably resistant to limited proteolysis, although a C-terminal 32-kDa segment could be removed from the full motor in a nucleotide-dependent manner by trypsin, resulting in altered enzymatic properties. Based on our findings we suggest a model in which both the stalk and the extreme C terminus of the dynein heavy chain control the rate-limiting step of product release in the dynein enzymatic cycle through long range allosteric mechanisms.

[1] Present address: Dept. of Gene Therapy and Regeneration Medicine, Gifu University School of Medicine, Gifu, 501-1194, Japan.
[2] To whom correspondence should be addressed. Tel.: 212-342-0546; Fax: 1-212-305-5498; E-mail: rv2025@columbia.edu.

MATERIALS AND METHODS

Protein Production—The 380-kDa motor domain fragment was cloned from Gly[1286]–Glu[4644] of rat cytoplasmic dynein into the baculo-virus expression vector pVL1393 (BD Biosciences) with a C-terminal in-frame hexahistidine tag. The 210-kDa fragment was subcloned from Gly[1286]–Glu[3106] of the 380-kDa construct into pVL1393. Hi5 cells were infected with virus for 40 h. The cells were washed and resuspended in phosphate-buffered saline, and the recombinant motor domain fragments were extracted from the cells by homogenization in extraction buffer (50 mM Pipes,[3] pH 7.2, 50 mM Hepes, 2 mM MgSO$_4$, 2 mM EGTA) supplemented with 1 mM dithiothreitol and protease inhibitor mixture (Sigma). The cytosolic extract was spun at $5000 \times g$ for 10 min and 100 000 $\times$ g for 30 min. The supernatant was applied to a Ni^{2+}-affinity column (Ni^{2+}-nitrilotriacetic acid superflow; Qiagen) equilibrated in extraction buffer supplemented with 20 mM imidazole. Unbound material was removed by washing with 16 volumes of extraction buffer supplemented with 10 mM imidazole, and the protein was eluted in 5 volumes of elution buffer (50 mM Pipes, pH 7.2, 50 mM Hepes, 2 mM MgSO$_4$, 2 mM EGTA, 125 mM imidazole, 1 mM dithiothreitol). Eluted protein was extensively dialyzed in extraction buffer to remove the imidazole. Protein concentration was determined by the Bradford method, using albumin as a standard. A typical batch of six 15-cm dishes of confluent Hi5 cells produced 2–4 mg of recombinant protein that had no visible sign of contaminants or degradation. Peak fractions were pooled, flash-frozen in liquid nitrogen, and subsequently stored at −80 °C.

Enzymatic Assays—ATPase activities were determined using the malachite green assay (13). ATPase activity was expressed as the number of ATP hydrolyzed per dynein motor fragment/s (s^{-1}) For microtubule-stimulated ATPase, 50 μl of taxol-stabilized microtubules (tubulin; Cytoskeleton) at a concentration of 5 mg/ml were pelleted at 90,000 $\times$ g for 30 min at 25 °C. The supernatant was saved for later SDS-PAGE analysis, and the pellet was resuspended in 20 μl of a sample containing the motor domain. Following a 30-min incubation, 2 mM ATP was added, and the reaction was continued for an additional 30 min. Control samples of motor domain fragment without microtubules and of microtubules alone were included in the analysis.

Vanadate inhibition of dynein ATPase activity was carried out in the presence of 2 mM ATP. UV-vanadate photocleavage was performed essentially as reported previously (7). A sample of recombinant motor fragment was incubated with 500 μM ATP and 500 μM vanadate for 1 h at room temperature and irradiated for 90 min on ice with UV light (365 nm). Vanadate-mediated photocleavage was determined by SDS-PAGE.

Solute Quenching and ADP Binding and Release Kinetics—The fluorescence emission of 2′-deoxy-mant-ADP bound to the 380- and 210-kDa fragments of dynein was measured as a function of acrylamide concentration as described previously (14). In brief, dynein fragments were mixed with a 10-fold molar excess of 2′-deoxy-mant-A DP, incubated overnight at 4 °C, and the excess nucleotide was removed by gel filtration on pre-poured Sephadex G-25 columns (PD-10, GE Healthcare), followed by dialysis. The fluorescence emission of the bound mant nucleotide was monitored in a steady state fluorimeter (ISS, Inc.) by exciting at 356 nm and monitoring the emission at 450 nm. Small aliquots of concentrated acrylamide were added, and the fluorescence intensity was measured during constant stirring. The effects of acrylamide quenching can be described by the Stern-Volmer Equation 1 (15),

$$\frac{F_0}{F} = \left(\sum_i \left(\frac{f_i}{1 + K_i[Q]\exp(V_i[Q])} \right) \right)^{-1} \quad \text{(Eq. 1)}$$

where F_0 and F are the fluorescence intensities in the absence and presence of quencher; f_i is the fractional emission of each component; K_i is the Stern-Volmer quenching constant, and V_i is the solute quenching (Q) parameter.

The kinetics of 2′-deoxy-mant-ADP release from the 380- and 210-kDa motor domain fragments were measured by mixing mant nucleotide-labeled dynein fragment in a stopped flow spectrometer (SX18.MV, Applied Photophysics, Ltd.) with 2 mM ATP. The resulting fluorescence transient was produced by excitation at 356 nm and observation at 90° through a 450 nm cut-off filter. Essentially identical results were obtained by excitation of the mant fluorophor through energy transfer from vicinal tryptophan residues (295 nm). The kinetics of 2′-deoxy-mant-ADP binding to a dynein-microtubule complex was monitored by mixing 10 μM tubulin + 2 μM 380-kDa fragment in the stopped flow spectrometer with 2′-deoxy-mant-ADP. Binding was monitored by exciting the mant fluorophor via dynein tryptophan residues (295 nm) and observing the resulting emission at 90° through a 450 nm cut-off filter.

Limited Proteolysis—Motor domain fragments were incubated with trypsin for 1 h at room temperature. Proteolysis was terminated by boiling in SDS-PAGE sample buffer for 5 min or by the addition of 1-chloro-3-tosylamido-7-amino-2-heptanone at a final concentration of 100 μM. The effect of nucleotides was determined by preincubation of the motor domain fragment for 1 h with 400 μM ATP plus 400 μM vanadate or 1 mM of either AMP-PNP, ADP-AlF$_3$, or ADP for 1 h followed by the addition of trypsin and incubation for an additional hour. Composition of the proteolytic products was analyzed by SDS-PAGE. N-terminal sequencing was carried out on electroblotted proteolytic fragments by automated Edman degradation on a 494 protein sequencer (Applied Biosystems) and by high pressure liquid chromatography fractionation. The C-terminal boundaries were deduced by measuring the masses of the proteolytic fragments using matrix-assisted laser desorption/ionization-time-of-flight mass spectrometry (Voyager-DE STR, Applied Biosystems). A matrix solution containing a 3:1:2 (v/v/v) mixture of formic acid/water/isopropyl alcohol was mixed with the proteolytic products, spotted onto a sample plate pretreated to form an ultrathin layer of matrix, and analyzed as described (16). Size-exclusion chromatography fractionation of the tryptic digest was carried out on a Superose 6 FPLC column (GE Healthcare) equilibrated with extraction buffer. Separation was conducted at a flow rate of 0.3 ml/min. Aliquots from each fraction of eluted digest were tested for ATPase activity and analyzed for fragment composition by SDS-PAGE.

RESULTS

Basal and Microtubule-stimulated ATPase Activities—To determine whether the 210-kDa half-motor and 380-kDa full motor domains had enzymatic activity, each fragment was tested for its ability to hydrolyze ATP. Most interestingly, the specific activity of the half-motor was ~6 times higher than that of the full motor (Fig. 1A). The range of activities for the half-motor was broad, ranging from ~3 to ~10-fold higher than the full motor domain, reflecting variations in specific activity among half-motor preparations. The addition of saturating amounts of taxol-stabilized microtubules to the 380-kDa dynein motor produced an almost 10-fold increase in ATPase activity (Fig. 1*B*), whereas no stimulation was detected for the 210-kDa fragment lacking the microtubule-binding domain (see Fig. 4*C* for the N- and C-terminal boundaries of the two motor domain fragments). The difference in ATP turnover rate between microtubule-bound and nonbound dynein and between the

---

[3] The abbreviations used are: Pipes, 1,4-piperazinediethanesulfonic acid; mant, *N*-methylanthraniloyl; 2′dmD, 2′-deoxy-mant-ADP; AMP-PNP, 5′-adenylyl-*β,γ*-imidodiphosphate.

FIGURE 1. **Basal and microtubule-stimulated steady state activities for the half- and full dynein motor domain.** *A*, the basal ATPase activities of the 210-kDa half-motor and 380-kDa full motor domain were 1.70 ± 0.67 and 0.34 ± 0.11 s^{-1}, respectively. Mean ± S.D. were calculated from five preparations of the 210-kDa fragment and 12 preparations of the 380-kDa fragment. *B*, in the presence of microtubules (*MTs*), the ATPase activity of the 380-kDa fragment increased from 0.30 ± 0.01 to 2.85 ± 0.03 s^{-1}, whereas the activity of the 210-kDa fragment was unchanged. Data for each experimental preparation was obtained from two individual measurements. *C*, steady state activity of the 210-kDa (●) and 380-kDa (○) motor domain fragments as a function of ATP concentration. Data for both fragments fit a hyperbolic curve from which V_{max} and K_m were obtained (TABLE ONE).
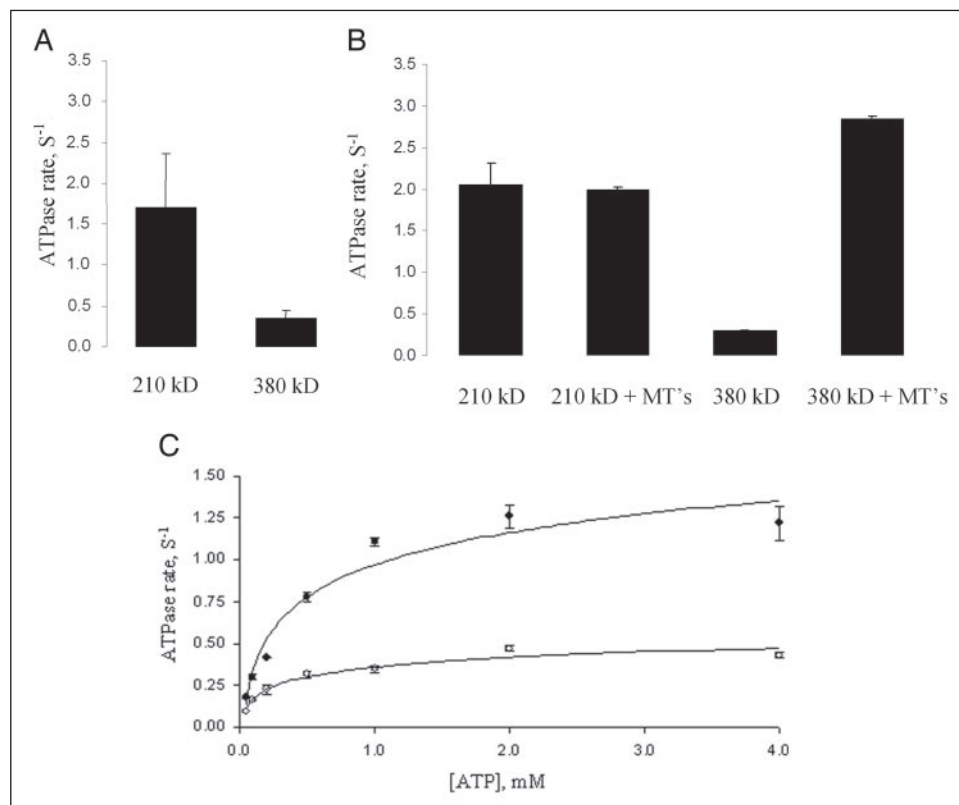
210- and 380-kDa fragment suggests that regions within the C-terminal half of the motor, including the microtubule-binding domain, are involved in controlling the rate by which dynein hydrolyzes ATP. To characterize V_{max} and K_m of the basal steady state ATPase of the two motor domain fragments, turnover rates were analyzed over a 100-fold range in ATP concentration (Fig. 1*C*). The V_{max} value of the 210-kDa fragment was about three times higher than that of the 380-kDa motor domain, whereas the apparent K_m value was ~50% higher (TABLE ONE), implying that the 210-kDa motor fragment binds and hydrolyzes nucleotides at greater efficiency.

Vanadate Photocleavage and Inhibition—Dynein, ADP, and vanadate form a stable, irreversible complex that mimics the ADP-phosphate intermediary state (7). In this state UV light irradiation causes a photolytic reaction that cleaves the dynein polypeptide chain at the first nucleotide-binding P-loop (5, 7). To test whether the 210- and 380-kDa dynein motor fragments were susceptible to photocleavage, the fragments were irradiated with UV light in the presence of ATP and vanadate. The treatment resulted in cleavage of the 380-kDa fragment at the first P-loop, whereas, surprisingly, no cleavage occurred for the 210-kDa fragment (Fig. 2A). To test whether the lack of UV cleavage reflected a decrease in affinity for vanadate, its ability to inhibit steady state ATPase activity was determined. Enzymatic activity of the 380-kDa fragment was strongly decreased by vanadate, with a 50% reduction in ATPase activity at ~0.1 μM vanadate and an 80% reduction at 2 μM vanadate (Fig. 2*B*), consistent with the sensitivity of the dynein holoenzyme to this inhibitor (7, 10). In contrast, the activity of the 210-kDa fragment was unaffected by vanadate (Fig. 2*B*), even at concentrations up to 250 μM. The combination of high ATPase activity and the insensitivity to vanadate suggest that the kinetics of nucleotide binding and hydrolysis were different in the truncated 210-kDa half-motor fragment compared with that of the entire 380-kDa motor domain.

Solute Quenching and ADP Binding Kinetics—These results suggested that the conformation of the catalytic site in the full motor domain is different from that of the 210-kDa half-motor domain. In particular, the increase in V_{max} for the half-motor domain may reflect weaker ADP binding, potentially reflected in a more solvent-exposed binding site in this fragment. In order to assess this possibility, we measured the accessibility of the fluorescent ADP analog, 2′-deoxy-mant-ADP (2′dmD), when bound to the full and half-motor domains. This was accomplished by exposure to acrylamide, a steady state fluorescence quencher. The plot of F/F_0 shows a single component for the Stern-Volmer quenching constant K for free 2′dmD and 2′dmD bound to the 210- and 380-kDa fragments with no appreciable component from static quenching. Furthermore, although the nucleotide in the 380-kDa motor domain fragment appears to be relatively buried in the protein ($K = 1.21 ± 0.12$ M^{-1}; Fig. 3A), the nucleotide-binding site in the 210-kDa fragment is considerably more accessible ($K = 2.00 ± 0.14$ M^{-1}). The value of K for free 2′dmD was $3.36 ± 0.14$ M^{-1}.

Product release is the rate-limiting step in the dynein mechanochemical cycle (17), and acceleration of ADP release is the basis for microtubule stimulation of its ATPase activity, at least for axonemal dynein (18). To provide further insight into the differences we observed in the steady state ATPase kinetics between the half-motor and full motor, the release rates of 2′dmD were measured by mixing a complex of 380-kDa-2′dmD or 210-kDa-2′dmD in the stopped flow with a large excess of ATP. In both cases, the resulting fluorescence transient from the displacement of the fluorescent nucleotide consisted of two well separated phases (data not shown). The amplitude ratio for the 380-kDa fragment was nearly 1:1, whereas it was closer to 2:1 for the 210-kDa fragment. The values of the corresponding rate constants are summarized in TABLE ONE. These results imply that both the 210- and 380-kDa motor domain fragments release ADP at two separate rates, consistent with nucleotide release from two separate ADP-binding sites. In the half-motor fragment, the two rate constants differed by a factor of 35, whereas in the full motor, the difference was smaller (~5–10 times; TABLE ONE). In addition, product dissociation from the 210-kDa frag-

TABLE ONE

Kinetic parameters for the 210-kDa half-motor and 380-kDa full motor domain fragments

The relative amplitudes for the two phases of ADP release are given in parentheses.

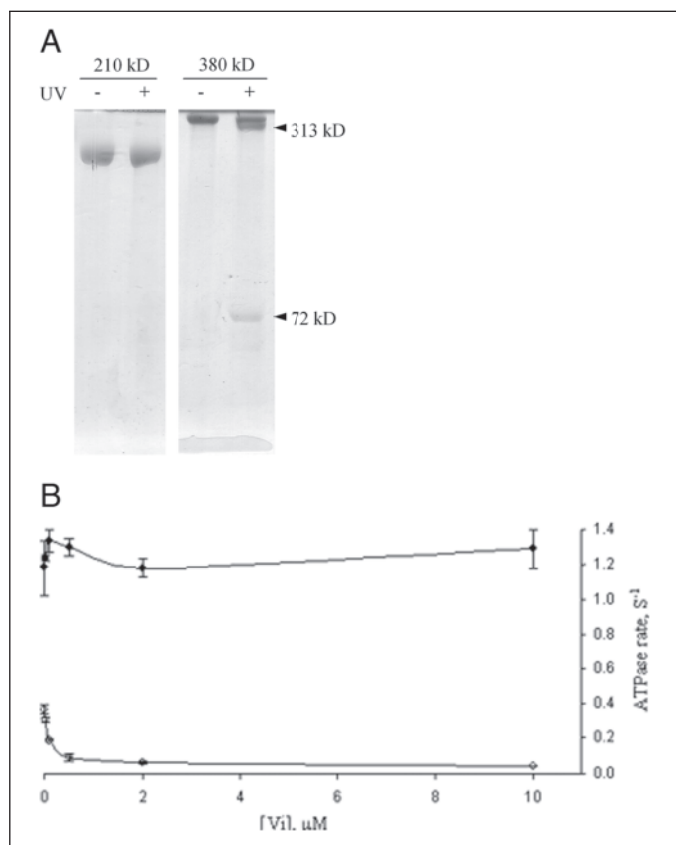|	ATPase V_{max}	ATPase K_m	ADP release rate
	s^{-1}	m_M	s^{-1}
210 kDa	1.42	0.39	3.80 (0.55); 0.11 (0.45)
380 kDa	0.49	0.26	0.035–0.060 (0.65); 0.006 (0.35)
380 kDa + microtubules			48.2; 9.1

FIGURE 2. **Vanadate-mediated photocleavage and ATPase inhibition of recombinant dynein fragments.** Effects of UV irradiation on ATP/vanadate-treated 210-kDa half-motor and 380-kDa full motor fragments. *A*, the 380-kDa motor was photolytically cleaved, and bands representing the resulting 313- and 72-kDa fragments are indicated (*arrowheads*). No apparent cleavage occurred for the 210-kDa fragment. *B*, vanadate inhibited steady state ATPase activity of the 380-kDa motor domain fragment (○) but not the 210-kDa fragment (●).

FIGURE 3. **Solvent accessibility and product release kinetics for recombinant motor domain in presence of microtubules.** *A*, 2'dmD fluorescence was measured in the presence of the 210-kDa (*blue dashed line*) or 380-kDa (*blue solid line*) motor domain fragments and in the absence of protein (*red solid line*). The three lines yielded Stern-Volmer quenching constants of 2.00 ± 0.14, 1.21 ± 0.12, and 3.36 ± 0.14 M^{-1} for the 210- and 380-kDa fragments and free 2'-deoxy-mant-ADP, respectively, and show that the 2'-deoxy-mant-ADP is much less accessible to solvent when associated with the 380-kDa *versus* the 210-kDa motor domain fragment. *B*, the 380-kDa motor domain-microtubule complex was rapidly mixed in the stopped flow spectrometer with 2'-deoxy-mant-ADP. Binding of 2'-deoxy-mant-ADP to the active site(s) of the recombinant dynein motor domain was monitored by energy transfer from dynein tryptophan residues to the mant fluorophor. The time course of the resulting fluorescence increase revealed two kinetic phases (data not shown) The rates obtained for the rapid (*blue*) and slow (*red*) phases (expanded in *inset*) are plotted as a function of 2'-deoxy-mant-ADP concentration, defining apparent second-order rate constants of 11.90 ± 0.20 and 0.40 ± 0.07 μM^{-1} s^{-1}. Extrapolation of the curves to the origin defines the apparent dissociation constants for the dissociation of 2'-deoxy-mant-ADP from dynein of 48.2 ± 7.7 and 9.1 ± 2.8 s^{-1}. The data reveal that two of the catalytic sites within the motor domain can be activated to release nucleotide by the presence of microtubules. Data for motor domain and half-motor domain alone were obtained by direct determination of 2'-deoxy-mant-ADP dissociation and are listed in TABLE ONE.

ment was ∼100 times faster than from the 380-kDa motor fragment (TABLE ONE). Taken together with the solvent accessibility studies (Fig. 3A), these results suggest that the nucleotide-binding site in the half-motor domain is more "open," resulting in enhanced solvent accessibility of the catalytic site, weaker coordination of nucleotide, and more rapid release of bound ADP.

For comparison with these results, we wished to monitor the effects of microtubules on the kinetics of ADP release from the 380-kDa motor fragment. This is difficult to accomplish directly, because of the low stability of the microtubule-dynein-ADP complex. Instead, we determined the rate of microtubule-activated ADP release indirectly, by measuring the kinetics of 2'dmD binding to a nucleotide-free complex of 380-kDa motor domain + excess microtubules. We combined the dynein-microtubule complex in the stopped flow with 2'dmD, and we monitored the rate of the resulting fluorescence increase as a function of nucleotide concentration. Under these conditions, the rate constants for the fluorescence increase due to 2'dmD binding to the two classes of catalytic sites should vary linearly with 2'dmD concentration, with the *y*
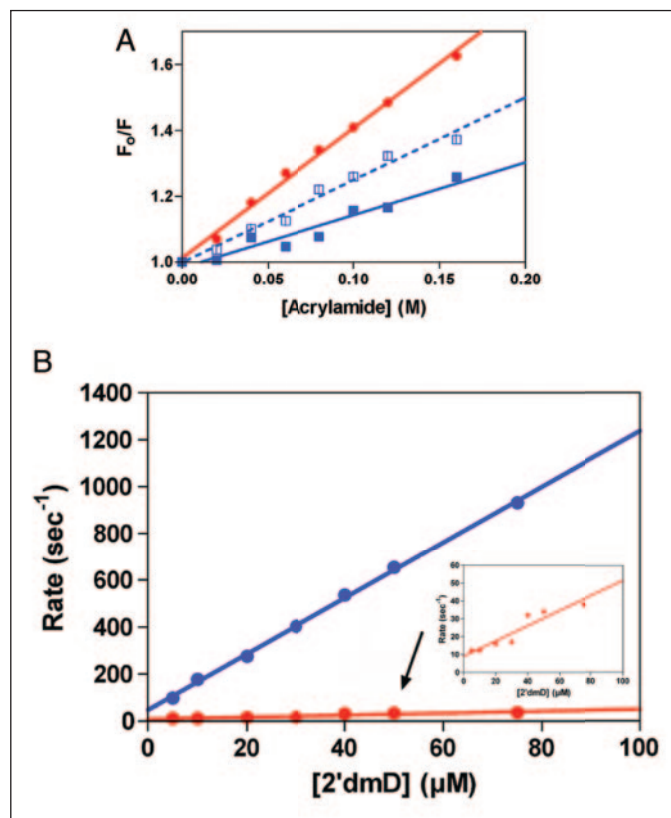
intercepts defining the apparent dissociation rate constants. As expected, the kinetics of the fluorescence increase due to 2'dmD binding in this experiment were biphasic, suggesting two exchangeable nucleotide-binding sites (data not shown). The rates of each phase varied linearly with [2'dmD], as expected (Fig. 3B). The apparent second-order rate constants for these two phases, defined by the slopes in Fig. 3B, were 11.90 ± 0.20 and 0.40 ± 0.07 $\mu M^{-1} s^{-1}$. Furthermore, the apparent dissociation rate constants, defined by the *y* intercepts of these plots, were 48.2 ± 7.7 and 9.1 ± 2.8 s^{-1}. These apparent dissociation
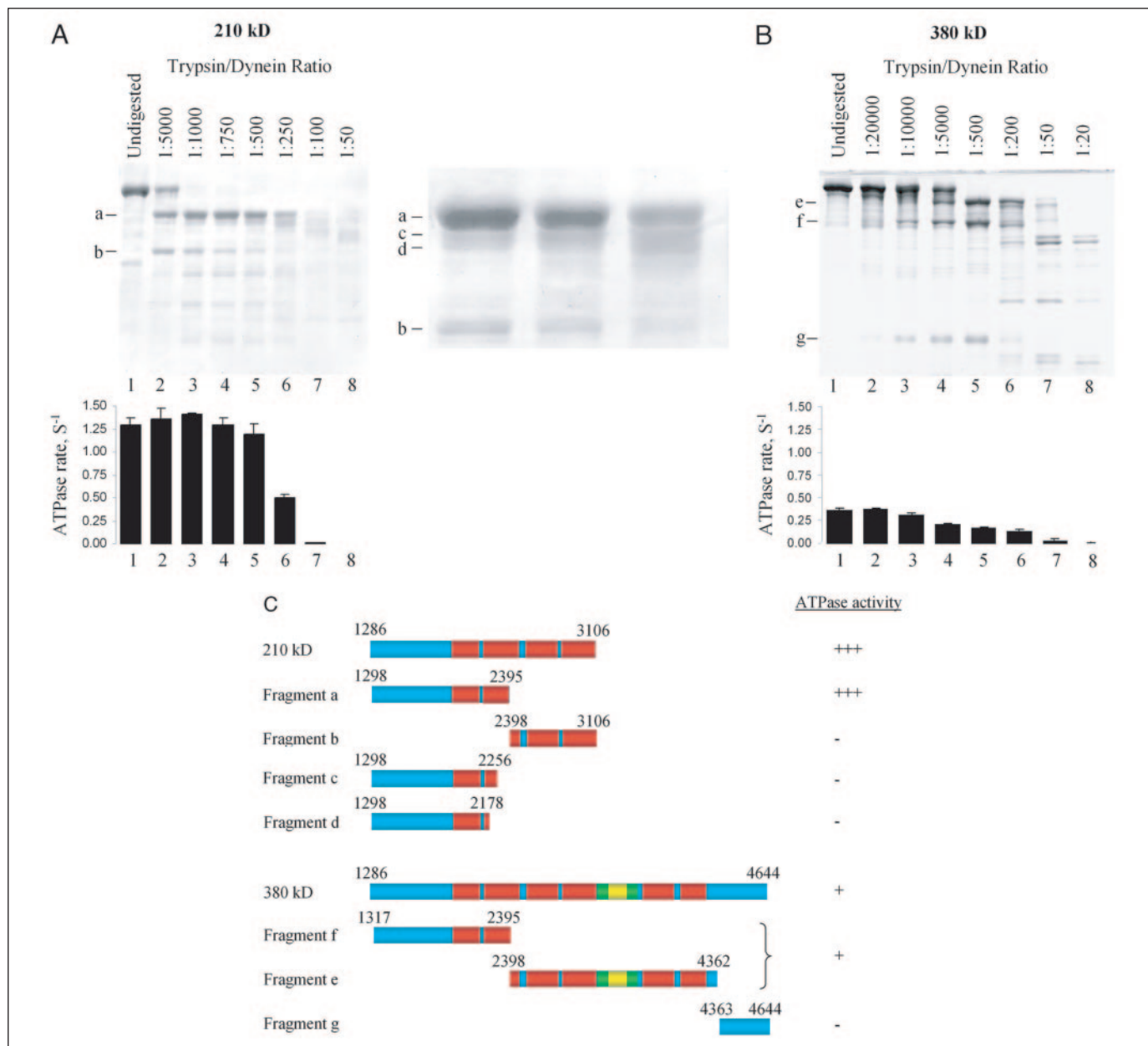
FIGURE 4. **Controlled proteolysis with trypsin.** Proteolysis was carried out on the 210-kDa half-motor and 380-kDa full motor domain fragments. *Top*, SDS-PAGE of digests obtained from proteolysis at various concentrations of trypsin. *A*, digestion series of 210-kDa fragment; an enlarged region of the electrophoretic gel (*box*) is shown for clarity (*inset*). *B*, digestion series of 380-kDa fragment. The major proteolytic fragments are denoted *a–g*. *Bottom*, ATPase activity of each digest. *C*, representation of the 210- and 380-kDa motor domain fragments and their proteolytic fragments based on N-terminal amino acid sequencing and mass spectrometry. The six AAA domains are labeled in *red* and the microtubule-binding stalk in *green/yellow*. The boundaries for each of the fragments denoted in *A* and *B* are indicated. Also shown are the ATPase activities for recombinant 210- and 380-kDa motor domain fragments and deduced relative activities for the tryptic fragments (see text). From the data in Fig. 5*B*, fragments *e* and *f* remain associated, as indicated by *brackets*.

rates compare with the rates of 0.035– 0.060 and 0.006 s^{-1} in the absence of microtubules (TABLE ONE) and suggest that ADP release is stimulated by microtubules in each of the exchangeable catalytic sites of the full motor domain, consistent with data from a recent mutational study on cytoplasmic dynein (8).

Proteolytic Analysis—As an additional means to gain insight into conformational and enzymatic control within the dynein motor domain, we subjected the 210- and 380-kDa motor domain fragments to controlled proteolysis. Proteolytic sites were identified by SDS-PAGE, N-terminal sequencing, and mass spectrometry. Proteolysis of the 210-kDa motor domain at a relatively low trypsin concentration generated two fragments: one from residues 1298–2395, which included the N-terminal segment AAA1 and two-thirds of AAA2 (Fig. 4, *A* and *C*, fragment a), and a smaller fragment from residues 2398 and 3106 that

includes the remainder of AAA2 and the entire C-terminal region (Fig. 4, *A* and *C*, fragment b). At a higher trypsin concentration, two additional fragments were produced, which were 139 and 217 residues shorter at the C-terminal end of fragment a, respectively (Fig. 4, *A* and *C*, fragments c and d).

Three major tryptic sites were identified within the 380-kDa full motor domain. Most interestingly, two of these sites at residues 1317 and 2398 were almost identical to those generated from the 210-kDa half-motor fragment (Fig. 4, *B* and *C*), indicating that the full and half-motor domain polypeptides are equally resistant to proteolysis and suggesting that they have similar structural stability. A third cleavage site at residue 4362 in the full motor domain generated a 32-kDa fragment from the C-terminal region of the dynein heavy chain (Fig. 4, *B* and *C*, fragment g) plus a fragment including part of
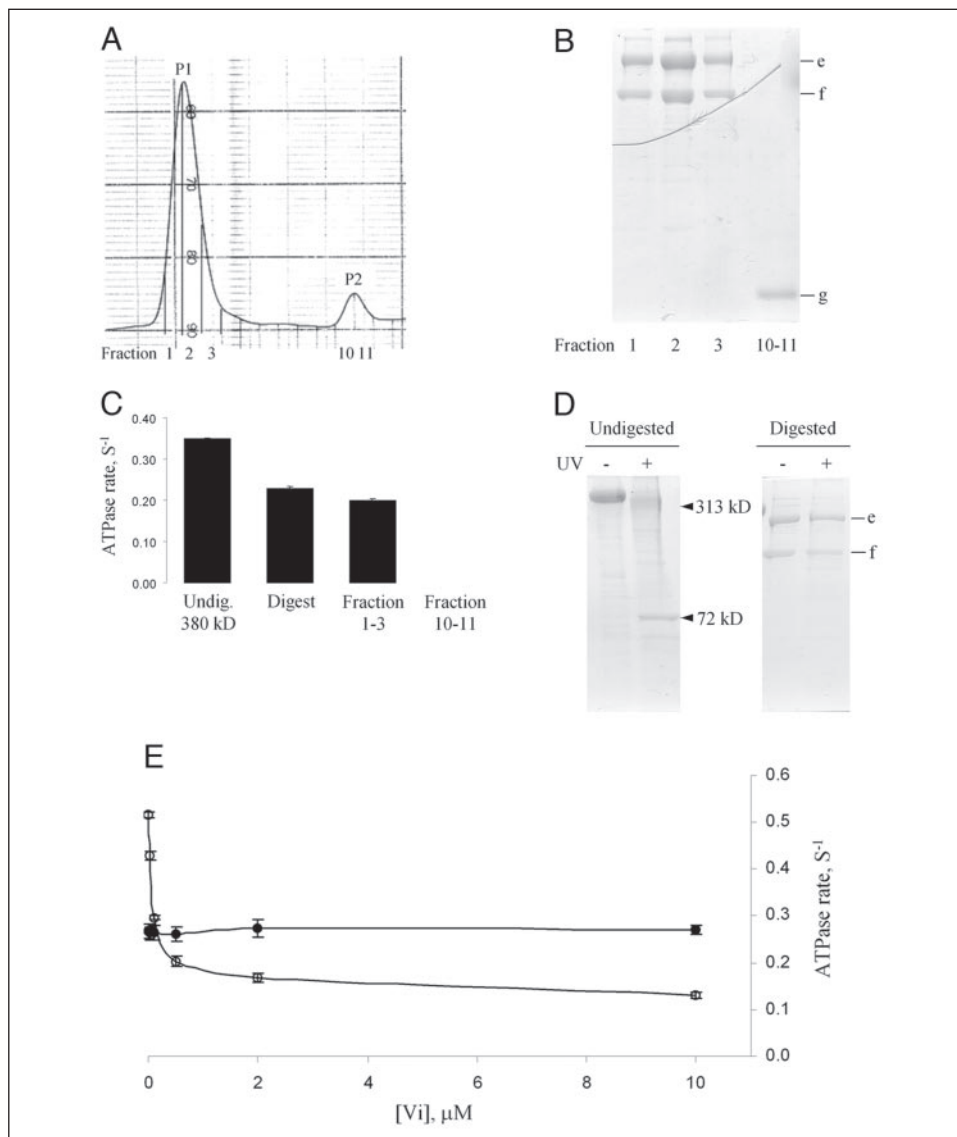
FIGURE 5. **Fractionation of tryptic digest by size-exclusion chromatography.** *A*, fast protein liquid chromatography fractionation of the 380-kDa dynein motor domain digest produced two peaks, *P1* and *P2*. *B*, Coomassie Blue-stained gel showing the relative content of tryptic *fragments e* and *f* in early (*lane 1*), middle (*lane 2*), and late (*lane 3*) eluting fractions from P1 and of *fragment g* in *fractions 10–11* of P2. *C*, ATPase activities of the undigested (*Undig.*) motor domain, the entire digest, and the fractionated digest. *D*, photocleavage experiments on undigested and digested 380-kDa motor domain with ($+$) and without ($-$) UV irradiation. *E*, vanadate inhibition of the undigested ($\bigcirc$) and digested ($\bullet$) 380-kDa motor domain fragment. Note the lower starting ATPase activity of the digest but complete lack of vanadate inhibition.

AAA2 and all of AAA3–AAA6, including the stalk (Fig. 4, *B* and *C*, *fragment e*).

In an attempt to establish which of the fragments were enzymatically active, ATPase activity was measured in digests generated at a series of trypsin concentrations. ATPase activity in digests of the half-motor domain was unaffected by proteolytic cleavage at residues 1298 and 2395, *i.e.* activity was unchanged at the point of complete digestion of the 210-kDa fragment (Fig. 4*A*). Activity was surprisingly stable over a substantial range of trypsin concentration but could ultimately be destroyed at a trypsin/dynein ratio of >1:500 (Fig. 4*A*). The drop in activity was correlated with the loss of fragment a and the generation of the 139- and 217-residue shorter fragments c and d (Fig. 4, *A* and *C*), suggesting that the two shorter fragments lack the ability to hydrolyze ATP, which likely reflects the loss of regulatory elements within AAA2 (see "Discussion"). Fragment b seemed less stable, and its loss was not obviously correlated with any further effect on enzymatic activity, suggesting that activity is associated entirely with fragment a. The pattern by which ATPase activity decreased in digests of the full 380-kDa motor domain differed from that of the half-motor domain. Proteolysis of the full motor produced a gradual decline in hydrolysis rate, and there was no obvious correlation with the degradation of fragment f (Fig. 4*B*).

Controlled proteolysis of the 210-kDa motor domain fragment using the relatively nonspecific proteases subtilisin and papain also generated a small number of stable fragments that were remarkably resistant to further proteolytic attack (see supplemental Fig. S1). The N-terminal boundaries for the three fragments (residues 1298, 1319, and 2415) were almost identical to those produced by tryptic proteolysis (residues 1298, 1317, and 2398).

Fractionation of the 380-kDa Motor Domain Tryptic Digest by Fast Protein Liquid Chromatography—To test the extent to which proteolysis of the 380-kDa motor domain affected the tertiary structure of the dynein motor domain, a tryptic digest was fractionated by size-exclusion chromatography. Two peaks were observed, a larger, symmetric peak and a smaller entirely resolved second peak (Fig. 5A). SDS-PAGE analysis of fractions from the early, middle, and late phase of the first peak showed that all three fractions contained both fragments e and f and that the fragments did not appear to be separated, suggesting that they were noncovalently associated (Fig. 5*B*). In contrast, the C-terminal proteolytic fragment was completely separated from the rest of the motor domain digest by the chromatographic procedure (Fig. 5*B*). To test whether removal of the C-terminal domain had an effect on ATPase activity, the activity from pooled fractions of the first peak and second peaks were compared with that of the entire digest and the intact 380-kDa fragment (Fig. 5*C*). The C-terminal fragment alone had, as expected, no ATPase activity. However, removal of the fragment by proteolysis and size-exclusion chromatography produced an approxi-

mate 40% drop in activity, comparable with that observed in the unfractionated digest. Our lab has reported previously that loss of ~400 residues from the C-terminal end of a recombinant dynein heavy chain fragment expressed in cultured vertebrate cells abolished vanadate-mediated photocleavage (5). To investigate whether tryptic removal of the 32-kDa C-terminal tryptic fragment produced a similar effect, the fractionated motor domain was subjected to vanadate-mediated photocleavage. When exposed to UV light in the presence of bound vanadate, the 380-kDa motor yielded fragments consistent with photocleavage at the P-loop of AAA1, whereas no visible sign of cleavage product was detected from the digest lacking the C-terminal piece (Fig. 5*D*). Consistent with this result, inhibition of ATPase activity by the digested motor domain was essentially abolished, even at very high vanadate concentrations (Fig. 5*E*). Together these results suggest that the C-terminal region affects and potentially controls the catalytic activity of AAA1.

Nucleotide Dependence of Tryptic Proteolysis—To examine the effect of nucleotide binding and hydrolysis on motor domain conformation, the 380-kDa motor fragment was incubated with the ATP analog AMP-PNP, the transition state mimic ADP-AlF$_3$, ATP/vanadate, or ADP and subjected to tryptic proteolysis. Analysis by SDS-PAGE showed that neither AMP-PNP nor ADP produced a change in the pattern of trypsin fragments. However, a novel large electrophoretic band was generated in the presence of ADP-AlF$_3$ or ADP-vanadate (Fig. 6*A*). SDS-PAGE analysis, N-terminal sequencing and mass spectrometry revealed that the band represented residues 2398–4644, *i.e.* it extended from the normal tryptic site in AAA2 all the way to the C terminus of the heavy chain (Fig. 6*B*, *fragment h*), indicating that proteolytic cleavage at residue 4362 had been reduced (although a decrease in the C-terminal fragment was less clear). This result suggests that a structural change occurs in the interface of AAA6 and the C-terminal domain, presumably as a result of a shift from a post- to a pre-force-producing state of the mechanochemical cycle (see "Discussion"). We also examined whether microtubule binding had a similar effect on cleavage at residue 4362, but no difference between bound and nonbound dynein was detected (data not shown).

DISCUSSION

To understand the mechanism by which production of force is coupled with ATP hydrolysis within the dynein motor, we produced a series of recombinant and proteolytic motor domain fragments, and we determined their enzymatic properties. A recombinant polypeptide consisting of AAA1–AAA4 exhibited a pronounced increase in ATPase activity relative to the full motor domain, with rates that in the most active preparations approached microtubule-stimulated levels. Both the recombinant 380-kDa full motor and 210-kDa half-motor domains are highly resistant to proteolysis, with no indication of cleavage between AAA units. Trypsin digestion did generate a 32-kDa C-terminal fragment of the full motor domain, production of which depends on the nucleotide-binding state of the motor domain. Loss of this fragment or deletion of the C-terminal half of the motor domain abolished sensitivity of the dynein ATPase to vanadate. Together, these results provide new insight into the functional organization of the motor domain and suggest novel features of ATPase regulation within the AAA ring.

Properties of Motor Domain Fragments—The N-terminal boundary of the motor domain fragments was selected based on results from previous experiments in our laboratory, which showed that the minimally sized fragment for vanadate-mediated photocleavage was framed by residues 1137 and 4644, the extreme C terminus of the heavy chain polypeptide (5). We observed tryptic cleavage at residues 1298 and 1317, 12 and 31 residues, respectively, from the N-terminal boundaries of the
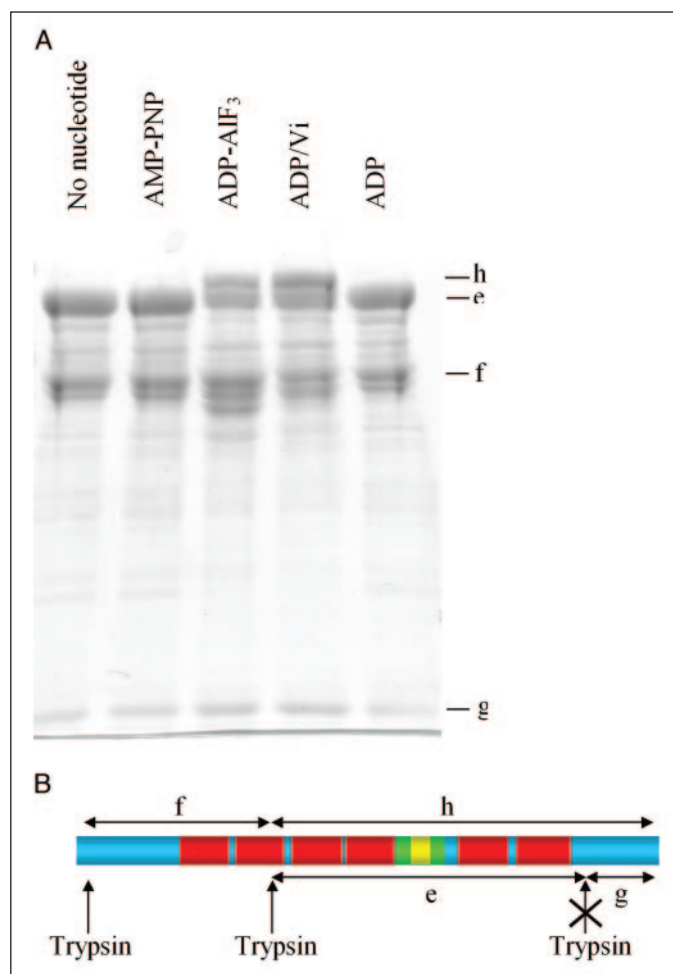
FIGURE 6. **Effect of nucleotides on tryptic proteolysis of 380-kDa motor domain fragment.** A, SDS-PAGE analysis of 380-kDa motor domain digests in the presence of nucleotide indicated. A novel large *fragment h* was generated only in ADP-AlF$_3$ or ADP-vanadate samples. B, boundaries of resulting fragments were determined by N-terminal sequencing and mass spectrometry and revealed specific inhibition by transition state nucleotides of tryptic digestion at residue 4362.

recombinant full motor and half-motor domain. The proximity of the cleavage sites to the end of the recombinant polypeptide suggests that we have properly identified a natural boundary between the stem and motor domain. Our boundary is similar to those used in ultrastructural analysis (19) and motor assays (20). Most interestingly, the C-terminal boundary for our half-motor fragment has proven to be close to what is now understood to be close to the juncture between AAA4 (21) and the stalk (5). Remarkably, our site also proved to be very close to the 13-residue overlap between the two component polypeptides of the unusual bipartite cytoplasmic dynein heavy chain from the corn smut Ustilago maydis (22). Again, these observations suggest that the C terminus of our half-motor resides at a natural structural boundary.

We identified two additional protease-sensitive regions with our recombinant polypeptide fragments, one within AAA2 and the other just following AAA6. Trypsin cleavage was detected within AAA2 at residue 2395 in both the full and half-motor fragments. The identity of this site provides strong evidence for the similarity in conformation and stability of the two recombinant polypeptides. Increased trypsin concentration yielded additional, slightly smaller fragments, which we analyzed in detail for the half-motor domain. We identified two additional cleavage sites within AAA2, at residues 2256 and 2178, 139 and 217 residues N-terminal to the 2395 site, respectively. Lys-2395 is located within a highly charged loop composed of an unusual combination of

amino acids, a cluster of five arginine and lysine residues followed by another cluster of five aspartic acid and glutamic acid residues. Although the unusual composition of this sequence implies that it may be of functional importance, it is not well conserved evolutionarily and is only found in cytoplasmic dynein in rodents and humans, and, oddly, in the ciliate *Trypanosoma*. Analysis of the polypeptide sequence within the second AAA domain suggests that the charged residues represent an extension of a loop unique to these cytoplasmic dyneins and that its accessibility at the surface of the molecule perhaps explains its sensitivity to proteolysis. However, as evidenced from size-exclusion chromatography and microtubule binding experiments, the fragments resulting from cleavage at Lys-2395 remained associated with each other, suggesting that trypsin only manages to nick the otherwise highly stable AAA ring. Subtilisin and papain generated N-terminal fragments of similar size to those generated by trypsin, with one papain cleavage site identified at residue 2415, 20 residues from Lys-2395. These results reveal that the central portion of AAA2 is accessible to proteases with diverse substrate specificities.

A third site of tryptic cleavage was identified at residue 4362, downstream of AAA6. The resulting C-terminal heavy chain fragment could be separated entirely from the rest of the motor domain. This feature implies that the site is located within a flexible interdomain junction, which may permit some degree of mobility to the C-terminal domain relative to the AAA ring. Potential further evidence for this model comes from three-dimensional reconstruction analysis of electron microscopic images of another cytoplasmic dynein motor domain. This study revealed a substantial gap between two of seven globular domains, which appeared, however, to be linked by a fine connector (19). Whether these structures actually correspond to the C-terminal domain characterized here remains to be determined. The C-terminal cleavage site became considerably less sensitive to proteolysis when the motor was occupied by ADP-ALF$_3$ or ADP-vanadate. These reagents are considered to mimic the ATP hydrolysis transition state and the post-hydrolysis and pre-power stroke states in the dynein mechanochemical cycle. Binding of ATP, AMP-PNP, or ADP, however, had no effect on the sensitivity to trypsin cleavage. These results provide a strong indication that the mobility of the C-terminal domain is dependent on the stage in the hydrolytic cycle of the rest of the motor domain. This conclusion is consistent with recent findings from structural analysis of the AAA protein p97/VCP, showing transition from a flexible to a rigid structure during hydrolysis to return to a more flexible state following product release (24).

We note that the entire N-terminal region of the motor domain fragments, an ~580 residue segment N-terminal to the AAA ring, together with AAA1 and part of AAA2, was strikingly resistant to trypsin, papain, and subtilisin. This result suggests that the portion of the dynein stem closest to the motor domain is itself extremely rigid, as is its junction with the AAA ring. We note that two-thirds of all conserved residues in the dynein heavy chain lie within this region plus AAA1 and AAA2.[4] Our observations therefore suggest that this entire region may function as a unit. The portion of the stem included in this region is of interest in the context of recent ultrastructural studies on a full-length flagellar dynein (12). Based on its position within the heavy chain, we speculate that this portion of the stem functions as so-called "linker" domain, a 10 nm long segment that was deduced to fold behind the AAA ring and generate the dynein power stroke. Our data argue that this region is not a simple mechanical lever attached to the ring by a hinge, as is the case in other motor proteins (25). Instead, we speculate that it functions with

AAA1 and AAA2 as the main catalytic core of the motor protein and is responsible for generating force.

Control of Enzymatic Activity within the Motor Domain—One of the greater surprises from this study was the potent ATPase activity of the recombinant 210-kDa half-motor domain. This result further substantiates the native-like behavior of the fragment. In addition, it appears to reveal a novel aspect of dynein motor domain enzymatic control in that the half-motor domain was far more active enzymatically than the full motor domain. The activity was more variable between preparations than was that of the full motor domain. The highest half-motor activity was very similar to that for the complete motor domain in the presence of microtubules. This result suggests that the C-terminal half of the motor domain acts as an endogenous inhibitor of the ATPase activity associated with AAA1–AAA4. Furthermore, this effect is likely to be attributable to the stalk in particular as the well established site for microtubule binding (5). Thus, we envision that the stalk suppresses ATPase activity and its removal or its interaction with microtubules relieves inhibition. We also examined the effects of vanadate on the half-motor domain. Vanadate-mediated UV photocleavage was abolished in this fragment, suggesting possible loss in vanadate affinity. This possibility was confirmed in ATPase inhibition experiments, which revealed a virtually complete loss of vanadate potency. This result and the increase in ATPase activity of the half-motor domain suggested a more general increase in active site accessibility. This hypothesis was borne out as judged by acrylamide quenching of mant-ADP fluorescence (Fig. 3A). Furthermore, the rate-limiting step of ADP release was dramatically increased, to levels close to those produced in the complete motor domain in the presence of microtubules.

Enzymatic analysis of protease-treated full and half-motor domains provided further insight into the intrachain control of ATPase activity. In the case of the half-motor domain, no apparent change in steady state ATPase activity was observed during trypsin digestion by the stage at which the initial electrophoretic band was completely degraded and production of the first stable tryptic fragment (residues 1298–2395) was complete (Fig. 4A). This result indicates that cleavage close to the extreme N terminus of the motor domain and at the initial AAA2 cleavage site did not affect ATPase activity. However, ATPase activity was lost with further digestion of this fragment at sites closer to the N terminus of AAA2. We note that the tryptic sites within AAA2 bracket the region containing a highly conserved putative arginine finger (residue 2356), a motif common to AAA family members (3). The arginine finger within AAA2 has been predicted to contact the bound nucleotide in AAA1 and to functions in stabilizing the negative charge in the ATP hydrolysis transition state (23). Therefore, we believe that the further tryptic sites at the N-terminal side of residue 2395, to produce fragment c (1298–2256) and fragment d (1298–2178), abrogate this interaction, resulting in the loss of hydrolytic activity in AAA1.

Cleavage of the full motor domain produced a reduction in its ATPase activity. At the stage of digestion by which the initial electrophoretic band had disappeared, ~50% of the ATPase activity was lost (Fig. 4B). Because cleavage of the half-motor domain at the N-terminal residue 1298 and the AAA2 residue 2395 had no effect on ATPase activity, as discussed above, we suspect that cleavage at the same or nearby sites in the complete motor domain would have little effect on its activity. That the products of cleavage at the AAA2 site 2395 remain associated with each other (Fig. 5B) further suggests that functional damage to the motor domain may indeed be minor. Based on these considerations, we argue that the effects on ATPase activity at this stage of the digestion of the full motor domain are more likely to result from loss of the C-terminal fragment. If this is the case, it provides insight into the function of this as yet unexplored region of the motor domain. First,
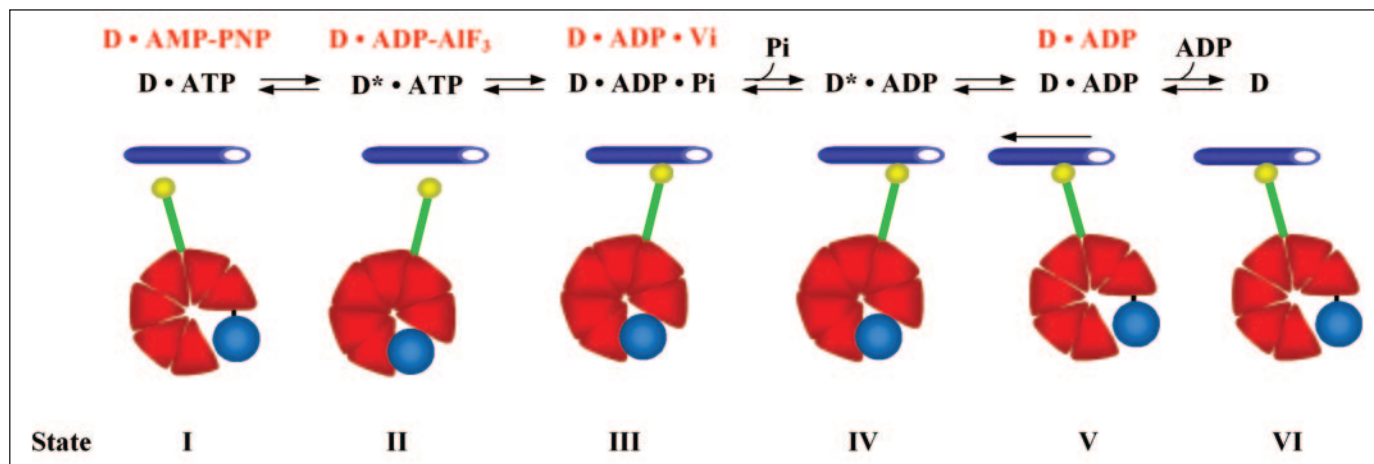

FIGURE 7. **A model for control of dynein ATPase.** The individual stages in the mechanochemical cycle of dynein have been identified by previous work on axonemal dynein (17, 18, 27), which may differ from cytoplasmic dynein. The nucleotide analogs (labeled in *red*) employed in our study are understood to trap the motor in each of the states indicated. The presence of either ADP-AlF$_3$ or ADP-vanadate eliminated tryptic cleavage at site 4362, suggesting that a substantial decrease in flexibility takes place at the interface of AAA6 and the C-terminal domain during hydrolysis (*state I* to *II*), which is reversed upon product release (*state IV* to *V*). The rate-limiting step of ADP release is divided in two steps (18), a high activity force-producing state following P$_i$ release (*state IV*) and a low activity state formed by ADP binding (*state V*). Based on our data, we propose a model in which both the stalk and the C-terminal domain serve to inhibit product release. In the case of the stalk, product release is stimulated by microtubule binding, a state mimicked by removal of the stalk. The physiological function of product release inhibition by the C-terminal domain is not known.

loss of the C-terminal domain alone cannot be responsible for the elevated steady state ATPase activity of the half-motor domain. If this were true, the initial stages of full motor domain digestion should result in a clear increase of ATPase activity, which is not observed. Instead, loss of the C-terminal domain appears to reduce ATPase activity. Most intriguingly, loss of this region also abolished vanadate-mediated photocleavage. This result again suggests a role for the C terminus in controlling entry and/or exit of substrate from the major ATPase sites within the motor domain.

Model for Control of ATPase Activity—Based on our enzymatic and kinetic data, which showed substantially higher rates of ATP hydrolysis and product release, and greater active site solvent accessibility in the truncated half-motor compared with that of the full motor domain, we propose a model in which elements within the C-terminal half of the dynein motor domain control catalytic activity by inducing conformational changes at the active sites within the AAA ring. As noted above, the properties of the half-motor domain fragment can be best understood as a consequence of the absence of the stalk. The considerable distance within the dynein heavy chain between AAA1 and the microtubule-binding stalk has been understood for several years to require some form of long range communication (5). ATPase mutations in AAA1 and AAA3 affect microtubule binding (5, 8, 11, 26). These observations suggest that communication between the microtubule binding and ATPase active sites occurs through AAA1–AAA4. Our current results provide the first evidence as to how the stalk affects ATPase activity. We propose that the stalk normally maintains AAA1 and AAA3 in a relatively closed conformation. Microtubule binding to the stalk, or removal of the stalk, initiated conformational changes, which are transmitted from AAA4 to AAA3 and AAA1. We cannot rule out transmission of conformational information from AAA5 through the C terminus to the active sites. However, this seems unlikely, as proteolytic removal of the C-terminal domain does not mimic the effects of microtubules or the complete ATPase behavior of the half-motor fragment.

The C-terminal domain has received little attention. We find that it is evolutionarily conserved in both cytoplasmic and axonemal dyneins. A possible exception is the yeast cytoplasmic dynein, which contains a truncated version of this domain. Although separated by some 2300 residues from the first P-loop, structural predictions for the dynein

motor domain place the C-terminal region close to the main hydrolysis site at AAA1, making interactions between the two structures possible. Proteolytic removal of the C-terminal fragment interfered with vanadate-mediated photocleavage at the first P-loop, a result consistent with our earlier work on the recombinant dynein heavy chain expressed in vertebrate cultured cells (5). Conversely, cleavage by trypsin at residue 4362 to generate the C-terminal fragment was reduced in the presence of ADP-AlF$_3$ or ADP-vanadate. This result indicates that the status of AAA1 and AAA3 alters the conformation of the AAA6 to C-terminal junction. To account for these observations, we propose that the C-terminal domain interacts directly with a site within the N-terminal half of the motor domain, most likely AAA1, although an interaction with the linker (12), *i.e.* the portion of the stem contiguous to AAA1, is also possible. We note that the nature of the interaction between the C- and N-terminal portions of the motor domain must change cyclically during each ATP hydrolysis event. This conclusion comes from the specific effect of ADP-AlF$_3$ and ADP-vanadate *versus* AMP-PNP, ADP, or the absence of bound nucleotide on trypsin accessibility. Thus, we predict that the AAA6 to C-terminal link becomes more rigid when AAA1 is in the pre-power stroke state, but not at other times during the dynein mechanochemical cycle. This model raises the possibility that the reciprocal effect of the C-terminal region on nucleotide binding by AAA1 is cyclic. Based on the insensitivity to vanadate photocleavage of dynein lacking the C-terminal domain, we propose that the C-terminal domain inhibits product release from AAA1 and AAA3 pending microtubule binding (Fig. 7). We do not yet know whether the reciprocal effects of AAA1 and the C-terminal domain occur sequentially or simultaneously, although they seem very likely to occur transiently. In all likelihood, the cycle of effects may correspond to a cycle of physical interactions, *e.g.* opening and closing of the motor domain ring, although this possibility remains to be tested. Based on our reasoning, it seems that the C-terminal domain provides an additional, and previously unsuspected, locus for control over the cross-bridge cycle, perhaps of relevance to the mechanism by which LIS1, NudEL, and other dynein modulators function.

REFERENCES

1. Dujardin, D. L., and Vallee, R. B. (2002) *Curr. Opin. Cell Biol.* **14,** 44–49
2. Hirokawa, N. (1998) *Science* **279,** 519–526
3. Neuwald, A. F., Aravind, L., Spouge, J. L., and Koonin, E. V. (1999) *Genome Res.* **9,** 27–43
4. Tynan, S. H., Gee, M. A., and Vallee, R. B. (2000) *J. Biol. Chem.* **275,** 32769–32774
5. Gee, M. A., Heuser, J. E., and Vallee, R. B. (1997) *Nature* **390,** 636–639
6. Gibbons, J. R., Gibbons, B. H., Mocz, G., and Asai, D. J. (1991) *Nature* **352,** 640–643
7. Gibbons, I. R., Lee-Eiford, A., Mocz, G., Phillipson, C. A., Tang, W. J., and Gibbons, B. H. (1987) *J. Biol. Chem.* **262,** 2780–2786
8. Kon, T., Nishiura, M., Ohkura, R., Toyoshima, Y. Y., and Sutoh, K. (2004) *Biochemistry* **43,** 11266–11274
9. Takahashi, Y., Edamatsu, M., and Toyoshima, Y. Y. (2004) *Proc. Natl. Acad. Sci. U. S. A.* **101,** 12865–12869
10. Shpetner, H. S., Paschal, B. M., and Vallee, R. B. (1988) *J. Cell Biol.* **107,** 1001–1009
11. Silvanovich, A., Li, M. G., Serr, M., Mische, S., and Hays, T. S. (2003) *Mol. Biol. Cell* **14,** 1355–1365
12. Burgess, S. A., Walker, M. L., Sakakibara, H., Knight, P. J., and Oiwa, K. (2003) *Nature* **421,** 715–718
13. Kodama, T., Fukui, K., and Kometani, K. (1986) *J. Biochem.* (*Tokyo*) **99,** 1465–1472
14. Rosenfeld, S. S., Correia, J. J., Xing, J., Rener, B., and Cheung, H. C. (1996) *J. Biol. Chem.* **271,** 30212–30221
15. Lehrer, S. S., and Leavis, P. C. (1978) *Methods Enzymol.* **49,** 220–236
16. Cadene, M., and Chait, B. T. (2000) *Anal. Chem.* **72,** 5655–5658
17. Holzbaur, E. L., and Johnson, K. A. (1989) *Biochemistry* **28,** 5577–5585
18. Holzbaur, E. L., and Johnson, K. A. (1989) *Biochemistry* **28,** 7010–7016
19. Samso, M., Radermacher, M., Frank, J., and Koonce M. P. (1998) *J. Mol. Biol.* **276,** 927–937
20. Nishiura, M., Kon, T., Shiroguchi, K., Ohkura, R., Shima, T., Toyoshima, Y. Y., and Sutoh, K. (2004) *J. Biol. Chem.* **270,** 22799–22802
21. Fan, J., and Amos, L. A. (2001) *J. Mol. Biol.* **307,** 1317–1327
22. Straube, A., Enard, W., Berner, A., Wedlich-Soldner, R., Kahmann, R., and Steinberg, G. (2001) *EMBO J.* **20,** 5091–5100
23. Mocz, G., and Gibbons, I. R. (2001) *Structure* (*Camb.*) **9,** 93–103
24. DeLaBarre, B., and Brunger, A. T. (2005) *J. Mol. Biol.* **347,** 437–452
25. Vale, R. D., and Milligan, R. A. (2000) *Science* **288,** 88–95
26. Reck-Peterson, S. L., and Vale, R. D. (2004) *Proc. Natl. Acad. Sci. U. S. A.* **101,** 1491–1495
27. Porter, M. E., and Johnson, K. A. (1983) *J. Biol. Chem.* **258,** 6582–6587